

**Photoresponse of KNbO₃–AF₂O₃ (A = Bi³⁺ or La³⁺)
ceramics and its relationship with bandgap narrowing**

ELICKER, Carolina, PASCUAL-GONZALEZ, Cristina, GULARTE, Luciano,
MOREIRA, Mario, CAVA, Sergio and FETEIRA, Antonio
<<http://orcid.org/0000-0001-8151-7009>>

Available from Sheffield Hallam University Research Archive (SHURA) at:
<https://shura.shu.ac.uk/18966/>

This document is the Accepted Version [AM]

Citation:

ELICKER, Carolina, PASCUAL-GONZALEZ, Cristina, GULARTE, Luciano,
MOREIRA, Mario, CAVA, Sergio and FETEIRA, Antonio (2018). Photoresponse of
KNbO₃–AF₂O₃ (A = Bi³⁺ or La³⁺) ceramics and its relationship with bandgap
narrowing. Materials Letters, 221, 326-329. [Article]

Copyright and re-use policy

See <http://shura.shu.ac.uk/information.html>

Photoresponse of $\text{KNbO}_3\text{-AFeO}_3$ ($\text{A} = \text{Bi}^{3+}$ or La^{3+}) ceramics and its relationship with bandgap narrowing

Carolina Elicker^{a,b,*}, Cristina Pascual-González^b, Luciano T. Gularte^a, Mario L. Moreira^a, Sergio S. Cava^a, Antonio Feteira^b

^a*Grupo de Pesquisa em Crescimento de Cristais Avançados e Fotônica, Universidade Federal de Pelotas, Pelotas, Brazil.*

^b*Christian Doppler Laboratory for Advanced Ferroic Oxides, Sheffield Hallam University, Sheffield, United Kingdom.*

* Corresponding author. *E-mail:* carolinaelicker@yahoo.com.br

Abstract

The crystal structure of $(1-x)\text{KNbO}_3\text{-}x\text{BiFeO}_3$ (KNBF) and $(1-x)\text{KNbO}_3\text{-}x\text{LaFeO}_3$ (KNLF) (where $x=0.00; 0.01; 0.02; 0.04; 0.08; 0.16; 0.32$) was evaluated by XRD and Raman spectroscopy. XRD data show the crystal symmetry to evolve from orthorhombic to tetragonal with increasing x . The optical *bandgap* was found to narrow systematically with increasing x . Raman spectroscopy analysis corroborated long-range polar order in all compositions. The photoresponse of $x=0.32$ shows a typical diode-like behaviour, with current and voltage of $0.115 \mu\text{A}$ and 0.075 V for KNBF and $0.19 \mu\text{A}$ and 0.035 V for KNLF, respectively. To our knowledge these represent the largest values among KNbO_3 -based ceramics, making them promising for photovoltaic applications.

Keywords: *KNbO_3 -based ceramics; bandgap narrowing; photoferroelectrics; ferroelectric photovoltaics.*

1. Introduction

The bulk photovoltaic effect in polycrystalline photoferroelectric materials it has long been believed to be associated with the crystal polarity of these materials. Nevertheless, recently Yang et al[1] suggested the bulk photovoltaic effect to actually originate from the non-centrosymmetry of ferroelectric semiconductors and to be independent of the ferroelectric polarization. Typically most ferroelectrics exhibit

bandgaps of 3 eV or higher, thereby absorbing in the UV range.[2]. Tailoring their *bandgaps* in order to achieve a maximum absorption around 1.5 eV, around the maximum of the solar spectrum, is therefore the ultimate goal[3].

Bandgap engineering of ferroelectric potassium niobate (KN) is being studied by some researchers. Pascual-González and co-workers[4] determined that the *bandgap* of $\text{KNbO}_3\text{--Bi(Yb,Me)O}_3$ (Me = Fe or Mn) narrowed by 1 eV for 95% $\text{KNbO}_3\text{--5%BiYbO}_3$. Later, the same authors found a narrowing from 3.25 to 2.25 eV for 75% $\text{KNbO}_3\text{--25%BiFeO}_3$ compared to pure KNbO_3 [5]. Yu and co-workers[6] studied the system $(1-x)\text{KNbO}_3\text{--}x\text{Ba}(\text{Co}_{1/2}\text{Nb}_{1/2})\text{O}_3$ and noticed *bandgaps* as low as 2.4 eV for $x = 0.5$. Grinberg and co-workers[7] studied the system $(1-x)\text{KNbO}_3\text{--}x\text{Ba}(\text{Ni}_{1/2}\text{Nb}_{1/2})\text{O}_3$ and observed reduction by more than 2 eV when increasing x . They also found short-circuit current and open circuit voltages of ferroelectric photovoltaic device built with sample $x=0.1$ to be controlled by induced polarization.

This work presents the synthesis of $(1-x)\text{KNbO}_3\text{--}x\text{BiFeO}_3$ (KNBF) and $(1-x)\text{KNbO}_3\text{--}x\text{LaFeO}_3$ (KNLF) ceramics, their characterization and, for the first time, their application as a light harvesters in ferroelectric photovoltaic (FEPV) devices.

2. Materials and methods

Pure KNbO_3 , $(1-x)\text{KNbO}_3\text{--}x\text{BiFeO}_3$ (KNBF) and $(1-x)\text{KNbO}_3\text{--}x\text{LaFeO}_3$ (KNLF) were synthesized by solid-state reaction using K_2CO_3 , Nb_2O_3 , Fe_2O_3 , Bi_2O_3 and La_2O_3 (Sigma-Aldrich, purity $\geq 99.00\%$, 99.90%, 99.99%, 99.99% and 99.99%, respectively) as precursor materials. Powders were weighed according the required molar ratios and mixed using a ball mill with Y-stabilized Zirconia balls and isopropanol (Sigma-Aldrich). Slurries were dried, sieved and calcined twice in air at 800°C for 4h. Finely milled powders were uniaxially-pressed into pellets under ~150 MPa and the green compacts were sintered in air at 1075°C (KN), 1085°C (KNBF) and 1100°C (KNLF ceramics) for 4 h.

Purity and crystal structure analysis were carried out by X-ray diffraction (PANalytical™ Empyrean XRD, $\text{CoK}\alpha_1$ radiation). Crystal structure and long-range polarization were evaluated by Raman spectroscopy (InVia, Renishaw, 532 nm solid state laser). *Bandgaps* were estimated from DRUV-Vis spectra (Shimadzu, UV-3600 Plus) using the Wood and Tauc approach. Finally, ferroelectric photovoltaic devices (FEPV) were fabricated with with a layout FTO/ferroelectric/electrolyte/Carbon/FTO, where FTO

is fluorine-doped tin oxide coated glass and the electrolyte is Redox-couple I^-/I_3^- . Carbon was painted directly onto the FTO coated glass and the ferroelectric layer was deposited by casting. I–V measurements were made under white light (210 – 1500 nm) (Ocean Optics, DH–2000) with a Keysight U2722A Source Measure Unit.

3. Results and discussion

Fig. 1(a-d) shows the room-temperature XRD data for KNBF and KNLF ceramics. Pure KN appears to be single-phase, with crystal symmetry described by the orthorhombic $Amm2$ space group. Undoped KN exhibits the typical peak splitting expected for an orthorhombic perovskite, but within the detection limits of the equipment, KNBF and KNLF display single peaks, as shown in Fig. 1(b,d). Nevertheless, those peaks are clearly asymmetric, ruling out a simple cubic symmetry, as also corroborated by the Raman spectra in Fig. 2. Indeed, KNBF up to $x=0.16$ and KNLF up to $x=0.08$ exhibit spectral features consistent with orthorhombic symmetry. In KNBF $x=0.32$, orthorhombic and tetragonal crystal symmetries coexist, in agreement with the recent work by Lennox and co-workers[8]. Similarly, for KNLF $x=0.16$, a secondary tetragonal phase is also present, which appears to be in broad agreement with the work by Kakimoto and co-workers[9].

Raman spectroscopy data shown in Fig. 2 corroborates the crystal symmetries suggested by the XRD data. The typical spectral features exhibited by orthorhombic and/or tetragonal polymorphs are visible in the spectra of all compositions, which can also confirm the occurrence of long-range polar order. In this work, modes in the Raman spectra of KNBF and KNLF were assigned according to the classical work of Shen and co-workers[10]. Within the resolution limits of the equipment, it is possible to observe, in the low- to mid- wavenumber region of pure KN spectra: a (i) sharp mixed mode – $A_1(TO)$, $B_1(LO)$, $A_1(LO)$ and $B_1(LO)$ – at 193 cm^{-1} ; (ii) Fano-type interference dip at 199 cm^{-1} ; (iii) broad $B_1(LO)$ mode centered at 250 cm^{-1} ; (iv) $B_1(LO)$ at 275 cm^{-1} ; (v) sharp mixed mode – $A_1(LO)$ and $A_1(LO)$ – at 294 cm^{-1} . Modes (i), (ii) and (v) are considered as "fingerprints" for long-range polar order. In the high wavenumber region it is possible to observe a (vi) $B_1(LO)$ mode at 533 cm^{-1} ; (vii) $A_1(LO)$ mode at 600 cm^{-1} and; (viii) $A_1(LO)$ mode at 834 cm^{-1} . KNBF ceramics present a broadening of the modes with increasing x , which can be associated with the increasing of lattice disorder. A new shoulder neighbouring the sharp mixed mode at 193 cm^{-1} also

emerges. This new mode may be associated with A–O vibrations, in particular, with nanometric clusters rich in K^+ cations[5]. In KNLF $x=0.04$ ceramics it is possible to observe a sharp mode at $\sim 280\text{ cm}^{-1}$, characteristic of the tetragonal polymorph[11]. For both KNBF and KNLF ceramics, the peak centered at 250 cm^{-1} shifts towards lower wavenumbers when increasing x , and a sharp mode emerges at $\sim 280\text{ cm}^{-1}$, consistent with the orthorhombic-to-tetragonal phase transition[11].

The indirect optical *bandgaps* listed in Table 1 for KNBF and KNLF were determined using the Tauc plots given in the Supplementary Information. Pure KN has a *bandgap* of $\sim 3.4\text{ eV}$. With increasing x , the *bandgap* narrows continuously, for both KNBF, reaching 2.5 eV for $x=0.32$ (*i.e.* 26.5% reduction), in agreement with the work by Pascual-Gonzalez and co-workers[5], whereas for KNLF $x=0.32$ the *bandgap* narrows reaches 2.6 eV (*i.e.* 23.5% reduction). For KN, the excitation through the *bandgap* is a charge transfer from the O 2p states at the top of valence band to the Nb 4d states at the bottom of the conduction band[6]. For KNBF and KNLF compositions, the substitution Nb^{5+} by lower valence Fe^{3+} may give rise to increased repulsion between the O 2p and Fe 3d states and thereby to a higher valence band maximum, *i.e.* narrow *bandgap*. Additionally the disorder brought by Fe ions due to Fe 3d states, also observed in high wavenumber region of the Raman spectra, which is sensitive to local depolarization provide by Fe 3d and Nb 4d hybridization, may create localized states into the *bandgap*.

FEPV devices were fabricated from KNBF and KNLF $x=0.16$ and 0.32 . Current-tension (I–V) curves obtained under dark and white light are shown in Fig. 3. Due to the non-linear electric behavior of the FEPV devices, they were assumed as diodes[12] with shunt resistance (R_P) and series resistance (R_S). While R_P can exist due to charge recombination and/or trapping, (R_S) of the system can be attributed to the resistance of the interfaces ferroelectric/electrodes[13]. KNBF $x=0.16$ exhibits low diode-like behavior (Fig 3a) with low open circuit voltage, 0.009 V and short circuit current of $0.12\text{ }\mu\text{A}$. KNLF $x=0.16$ (Fig. 3c) appear to have a linear dependence current/tension. Measured short circuit current and open circuit voltage were $0.08\text{ }\mu\text{A}$ and 0.00022 V , respectively. Such linear behavior presented by both $x = 0.16$ indicates low R_P and high R_S , indicating that an enhancement in the interfaces ferroelectric/electrodes may lead to an improvement of the FEPV device response. Particularly, for both $x = 0.32$ (Fig. 3b,d), the I–V curves presented expected diode-like behavior, with low open circuit voltages and linear behavior in photocurrent region (Fig. 3b,d, *inset*). Measured short circuit current and open circuit voltage were $0.115\text{ }\mu\text{A}$ and 0.075 V for KNBF and $0.19\text{ }\mu\text{A}$ and 0.035 V for KNLF. Changing to the shape of the I–V curves

with increasing x can be related to the presence of the tetragonal phase. Also the bandgap narrowing is a reasonable explanation for photocurrent enhancement. This subject, however, needs further investigation.

4. Conclusions

It was demonstrated that the *bandgap* of KNBF and KNLF can be systematically narrowed by 0.9 eV (*i.e.* ~26.5% reduction) via replacement of K and Nb by Bi or La and Fe, respectively, without losing long-range polar order. I–V measurements revealed 0.68KNbO₃–0.32BiFeO₃ and 0.68KNbO₃–0.32LaFeO₃ to have diode-like behavior expected for solar cells. Moreover, KNBF and KNLF present higher values of current compared to previous works in the literature[7]. Hence they are promising for photovoltaic and optical sensor applications and require in-depth investigation.

Acknowledgements

The authors are thankful to CNPq, CAPES and FAPERGS, Grant Number 16/2551-0000525-7 for financial support. Carolina Elicker acknowledges CNPq for a SWE Scholarship (process no. 201665/2015–8). Cristina Pascual-González acknowledges Sheffield Hallam University for a VC doctoral scholarship. Antonio Feteira is thankful to CNPq for a Special Visiting Researcher Fellowship. Giorgio Schileo is acknowledged for the reflectance measurements. Cristian D. Fernandes is acknowledged for sharing his expertise on I–V measurements.

References

- [1] M.M. Yang, Z.D. Luo, D.J. Kim, and M. Alexe, Appl Phys Lett 110, (2017)183902.
- [2] Y. Yuan, Z. Xiao, B. Yang, J. Huang, J Mater Chem A. 17 (2014) 6027-41.
- [3] C. Paillard, X. Bai, I.C. Infante, M. Guennou, G. Geneste, M. Alexe, J. Kreisel, B. Dkhil, Adv Mater. 26 (2016) 5153-68.
- [4] C. Pascual-Gonzalez, G. Schileo, A. Feteira, Appl Phys Lett. 13 (2016) 132902.

- [5] C. Pascual-Gonzalez, G. Schileo, S. Murakami, A. Khesro, D. Wang I. M. Reaney, A. Feteira, Appl Phys Lett. 17 (2017) 172902.
- [6] L. Yu, J. Jia, G. Yi, Y. Shan, M Han, Mater Lett. 2016;184:166-168.
- [7] I. Grinberg, D.V. West, M. Torres, G. Gou, D.M. Stein, L. Wu, G. Chen, E.M. Gallo, A.R. Akbashev, P.K. Davies, J.E. Spanier, Nature. 503 (2013) 509-512.
- [8] R.C. Lennox, D.D. Taylor, L.J.V. Stimpson, G.B. Stenning, M. Jura, M.C. Price, E.E. Rodriguez, D.C. Arnold, Dalton Trans. 44 (2015) 10608-10613.
- [9] K.I. Kakimoto, I. Masuda, H. Ohsato, J Eur Ceram Soc, 25 (2005) 2719-2722.
- [10] Z. Shen, Z. Hu, T. Chong, C. Beh, S. Tang, M. Kuok, Phys Rev B. 52 (1995) 3976-3980.
- [11] J. Baier-Saip, E. Ramos-Moor, A. Cabrera, Solid State Commun. 135 (2005) 367-372.
- [12] Y. Liu, A. Hagfeldt, X.R. Xiao, S.E. Lindquist, Sol Energy Mater Sol, 1998;55:267-281.
- [13] J.S. Agnaldo, J.B.V. Bastos, J.C. Cressoni, G.M. Viswanathan, Rev Bras Ens Fis. 28 (2006) 77-84.

Figure Captions

- Figure 1 – X-ray diffractograms for KNBF and KNLF ceramics (a,c) and detailed peaks (b,d).
- Figure 2 – Room-temperature Raman spectra for KNBF (a) and KNLF (b) ceramics.
- Figure 3 – I–V curves for KNBF $x = 0.16$ (a), KNBF $x = 0.32$ (b), KNLF $x = 0.16$ (c) and KNLF $x = 0.32$ (d). Insets in each figure show detailed curves.

Table Caption

Table 1 - Indirect optical *bandgaps* for KNBF and KNLF ceramics.

Composition	Bandgap (eV)
KN	3.40
KNBF $x = 0.01$	3.13
KNBF $x = 0.02$	3.12
KNBF $x = 0.04$	2.70
KNBF $x = 0.08$	2.60
KNBF $x = 0.16$	2.55
KNBF $x = 0.32$	2.50
KNLF $x = 0.01$	3.21
KNLF $x = 0.02$	3.20
KNLF $x = 0.04$	2.70
KNLF $x = 0.08$	2.68
KNLF $x = 0.16$	2.58
KNLF $x = 0.32$	2.60

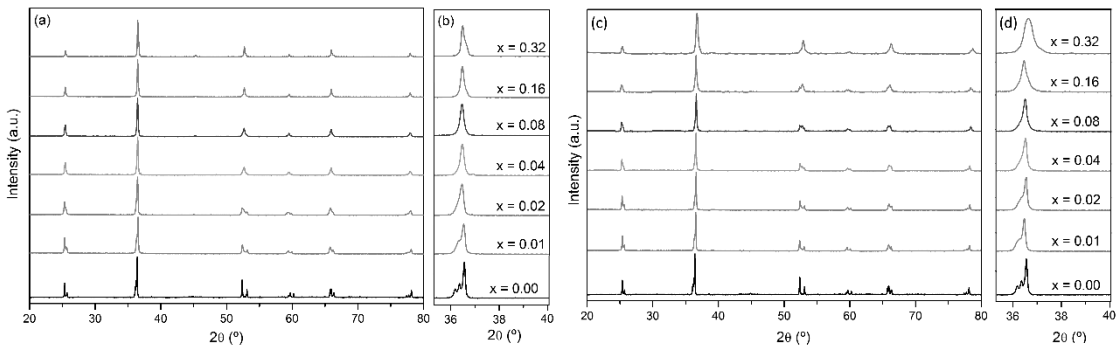


Fig. 1

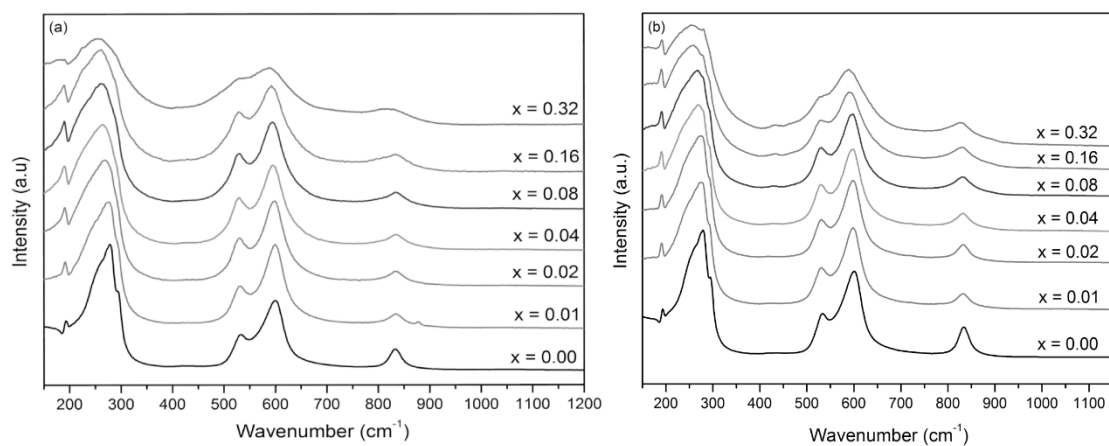


Fig. 2

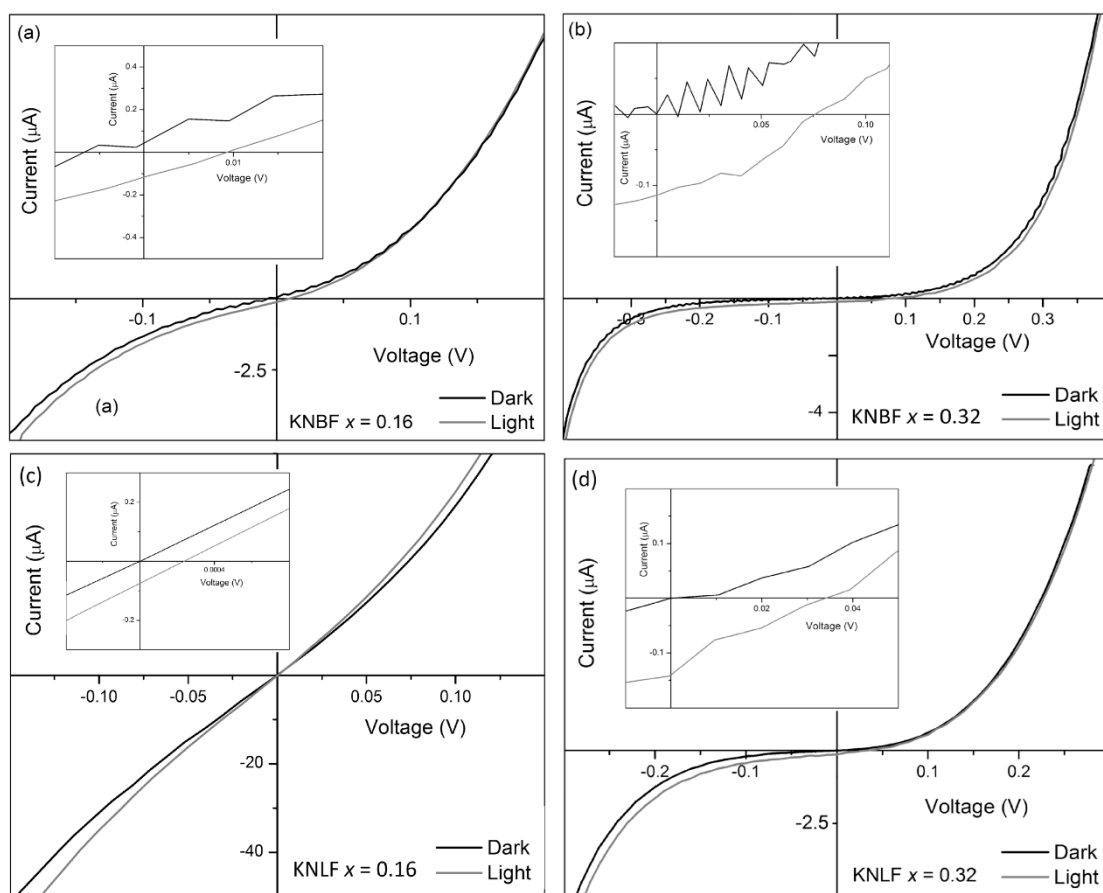


Fig. 3